ADVANCED ELECTRONIC MATERIALS
Open Access

Supporting Information

for *Adv. Electron. Mater.*, DOI 10.1002/aelm.202300732

Real-Time and Continuous Monitoring of Brain Deformation

Ziwei Liu, Chengqiang Tang, Jianzheng Li, Yiqing Yang, Wenjun Li, Jiajia Wang, Sihui Yu, Chuang Wang, Yajie Qin, Qi Tong, Xuemei Sun and Huisheng Peng**

Supporting Information for

Real-Time and Continuous Monitoring of Brain Deformation

Ziwei Liu[1]†, Chengqiang Tang[1]†, Jianzheng Li[2], Yiqing Yang[1], Wenjun Li[1], Jiajia Wang[1], Sihui Yu[1], Chuang Wang[1], Yajie Qin[2], Qi Tong[3], Xuemei Sun[1] and Huisheng Peng[1]**

[1]State Key Laboratory of Molecular Engineering of Polymers, Department of Macromolecular Science, Institute of Fiber Materials and Devices, and Laboratory of Advanced Materials, Fudan University, Shanghai 200438, China.

[2]School of Information Science and Technology, Fudan University, Shanghai 200438, China.

[3]Department of Aeronautics and Astronautics, Fudan University, Shanghai 200433, China.

†These authors contributed equally.

**Correspondence: sunxm@fudan.edu.cn, penghs@fudan.edu.cn.*

This file includes:

Materials and Methods

1. Materials and chemicals

Polydimethylsiloxane (PDMS, ELASTOSIL® RT 601 A/B) was purchased from WACKER Chemie Company. Dopamine hydrochloride (D103111) and poly(vinyl alcohol) (PVA, 1799) were purchased from Shanghai Aladdin Biochemical Technology Co., Ltd. Dextran (31392) was purchased from Sigma-Aldrich (Shanghai) Trading Co., Ltd. The diazo sensitizer was purchased from Denbishi Fine Chemical (Kunshan) Co., Ltd. Tris-HCl (1.5 M, pH = 8.8, E8028) and agarose (89283C) were purchased from Adamas-beta Co., Ltd. 0.01 M Phosphate-buffered saline (PBS, G4202), paraformaldehyde fixative (G1101), Anti-NeuN Mouse mAb (GB13138-1), Anti-GFAP Rabbit pAb (GB11096), Alexa Fluor® 488-conjugated Goat Anti-Mouse lgG(H+L) (GB25301), Cy3 conjugated Goat Anti-Rabbit lgG(H+L) (GB21303), and 4',6-diamidino-2-phenylindole (DAPI, G1012) were purchased from Solarbio Science and Technology Co., Ltd. Dental adhesive resin cement (Super-Bond C&B) was purchased from SUN MEDICAL Co., Ltd. All other reagents were purchased from Sinopharm Chemical Reagent Co., Ltd.

2. Instruments

The electrodes of brain deformation sensor (BDS) were patterned through a direct-write optical lithography system (Microwriter ML3, Durham Magneto Optics Ltd.), thermal evaporator (FS380-S8, FANGSHENG Co., Ltd.) and reactive ion etch system (Phantom III, Trion Technology Co., Ltd.). The structure of BDS was characterized through scanning electron microscopy (SEM, TESCAN VEGA 3 XMU). The detachment test and the sensing performance *in vitro* were performed by the table-top universal testing instrument (HY0350, Shanghai HengYi precision instruments Co., Ltd.). The rapid dynamic tracking ability was characterized by a load frame Instrument (Electroforce 3200, TA Instruments–Waters LLC Co., Ltd.). The polydopamine (PDA) layer was characterized by atomic force microscopy (FastScan, Bruker Co., Ltd.) and Raman microscopy (inVia Qontor/NTEGRA Spectra II, Renishaw Co., Ltd. and NT-MDT Co., Ltd.). The rat experiments were carried out through the stereotaxic device (RWD Life Science Co., Ltd.). The capacitance signals were recorded by the printed circuit board (PCB). The coronal sections were observed through fluorescence microscopy (BX51, Olympus Co., Ltd.). The electrocardiograph was obtained by electrocardiograph monitoring system (YAN-6000, Yuyan Instruments Co., Ltd.). The end-tidal carbon

dioxide wave was obtained by Model C500 mainstream $ETCO_2$ module (Zhejiang National Medical Co., Ltd.).

3. Preparation of the electrode of BDS

The Si wafer was treated with oxygen plasma at 150 W for 2 min. The dextran aqueous solution (5 wt%) was spin-coated on the oxygen plasma-treated Si wafer as the sacrificial layer. The insulating layer was made of the PDMS (base polymer:crosslinker 10:1 weight ratio) solution diluted in the mixed solvent (hexane:ethyl acetate 4:1 volume ratio) by spin coating at a speed of 7000 r.p.m. for 30 s, and then annealing at 70 °C for 30 min. Au layer (20 nm) was deposited on the insulating layer through thermal evaporation. The 5 wt% diazo (relative to PVA) was dissolved in 7 wt% PVA aqueous solution to obtain the photoresist. The photoresist was spin-coated on the Au layer at a speed of 3000 r.p.m. for 30 s and exposed at the exposure dose of 200 mJ cm^{-2}. The deionized water at 60 °C was used for development. The pattern of the photoresist (2 mm × 2 mm) was transferred to the first PDMS layer and Au layer through reactive ion etching (CF_4, 40 mT, 150 W, 400 s). The second PDMS layer was spin-coated and cured in the same way. The second photolithography step was the same as above, which developed the larger pattern (4 mm × 4 mm) on the second PDMS layer. Reactive ion etching (CF_4, 40 mT, 150 W, 300 s) was used to transfer the larger pattern to the second PDMS layer. The Si wafer was immersed in water to release the electrodes. The density was calculated based on the Au electrode area of 2 mm × 2 mm in the center.

4. Preparation of PDA-modified electrode

The electrodes were immersed in the dopamine solution (2 mg mL^{-1}) for 4 h, which was prepared by dopamine hydrochloride dissolving in 0.1 vol% Tris-HCl aqueous solution.

5. Detachment test of the PDMS with/without PDA

The Si wafer was treated with oxygen plasma at 150 W for 2 min. 5 wt% dextran aqueous solution was spin-coated as the sacrificial layer. Polyimide (PI) tape was attached around the Si wafer as a frame (internal area: 2.5 cm × 2.5 cm), the PDMS film was made as described above. The Si wafer was immersed in water to release the PDMS film with the PI frame, and then transferred to the 2 cm × 2 cm × 2 mm hollow foam frame as the PDMS without PDA sample. The Si wafer directly immersed in the dopamine solution was the PDA-modified PDMS sample. The samples were in contact

with the fresh rat brain surface for 10 min at the same height, then the frames were lifted (2 mm min^{-1}) by HY0350 Table-top Universal Testing Instrument until the films peeled off the brain.

6. Design of the PCB for capacitance detection

The mainly wireless electronics consisted of the BLE SoC (Nordic 52840) for wireless communication, and the AFE SoC (AD5933) was used to measure BDS responses, which exhibited a detection range from 0.1 to 2 pF. The sampling rate of the entire system was 100 Hz. BLE SoC with 64 MHz Arm Cortex-M4F CPU was used to communicate with AD5933 through I2C and transmitted data to the host computer *via* Bluetooth. The AD5933 was a high-precision capacitance converter system that combined an on-board frequency generator with a 12-bit, 1 MSPS, analog-to-digital converter (ADC). The frequency generator allowed an external capacitance to be excited with a known frequency. The signal was sampled by the on-board ADC and a discrete Fourier transform (DFT) was performed by an on-board DSP engine. Moreover, in order to improve the measurement accuracy of the whole system, an external resistance of the same magnitude was utilized to calibrate the whole system before measurement.

7. Implantation of BDS

The rats (SD, male, 6−8 weeks) were purchased from Shanghai SLAC Laboratory Animal Co., Ltd. The animal experiments were conducted in accordance with the approval number of SYXK2020-0032 published by the Animal Experimentation Committee of Fudan University. All the treatments for animals were guided by the National Institutes of Health and Fudan University. After disinfection treatment, the rat was fixed on the stereotaxic device by ear rods while anesthetized with 2.0% isoflurane ($V_{isoflurane}$:V_{air}). The scalp was cut with surgical scissors, and then fixed with hemostatic forceps. The connective tissue and periosteum were removed with scalpels to expose the skull. A 2 mm × 2 mm square was positioned with bregma as the center, and the skull of the square was removed by a cranial drill. The bottom electrode was placed on the brain tissue with the PDA-modified side in contact with the rat brain. The area with the Au layer (2 mm × 2 mm) was attached to the surface of brain tissue, and the edge of the electrode was fixed to the skull around the square by dental adhesive resin cement to make the area with the Au layer a groove. The top electrode was placed in the position corresponding to the bottom electrode as part of the skull. The leads of two electrodes

were exposed, and the other area was coated with dental adhesive resin cement.

8. *In vivo* monitoring of brain deformations

The leads were connected to the flexible printed circuit of the measuring module for brain deformation monitoring. For tests under different isoflurane concentrations, the rat was anesthetized with 1.0%, 1.5% and 2.0% isoflurane. The test was conducted 10 minutes after each adjustment of the anesthetic concentration to ensure that the rat reached a stable state. For continuous monitoring, the time to adjust the isoflurane concentration was recorded.

9. Brain tissue sections and immunofluorescence staining

BDS was implanted at the left parietal bone. After implantation for 2 weeks, the rat was sacrificed, and then removed the whole brain tissue into the paraformaldehyde. After the dehydration treatment, the brain tissue was embedded in paraffin and cut into ~3 μm slices to the further staining. For the staining of neurons and astrocytes, the neuronal nuclei protein (NeuN, 1:8000) and glial fibrillary acidic protein (GFAP, 1:500) were used as the primary antibodies, Cy3 conjugated Goat Anti-Rabbit lgG (H+L) (1:300) and Alexa Fluor® 488-conjugated Goat Anti-Mouse lgG (H+L) (1:500) were used as secondary antibodies. 4’6-diamidino-2-phenylindole (DAPI) was used for the staining of all the nuclei.

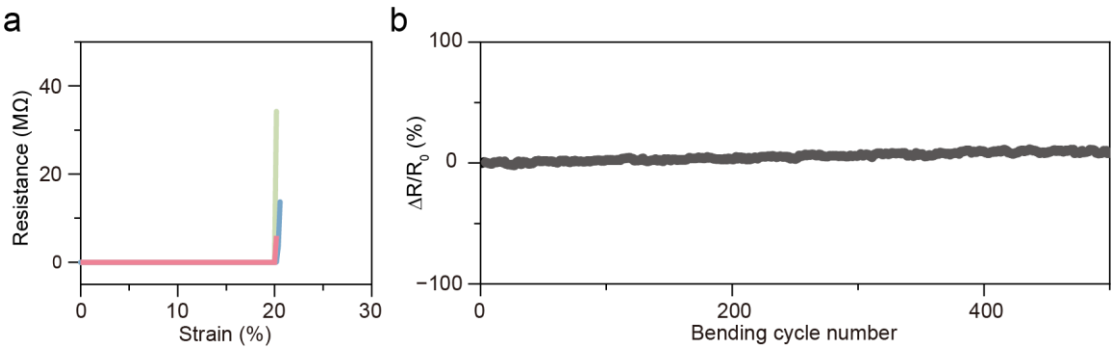

Figure S1. Electrical stability of BDS. a) The resistance of BDS under stretching. Typical three samples were shown. b) The resistance change of BDS under cyclic bending.

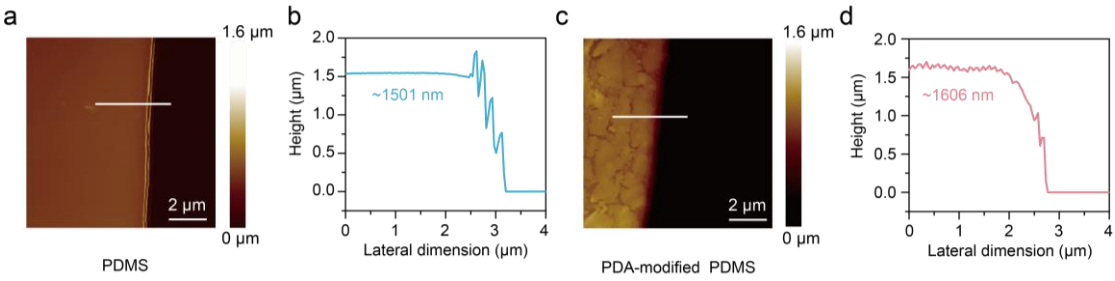

Figure S2. AFM images and height variations of bare PDMS and PDA-modified PDMS films. a) and b) AFM image of the bare PDMS film on Si wafer and the height variation of the white line (1501 nm). c) and d) AFM image of the PDA-modified PDMS film on a Si wafer and the height variation of the white line (1606 nm). The average height difference was the thickness of the PDA (~100 nm).

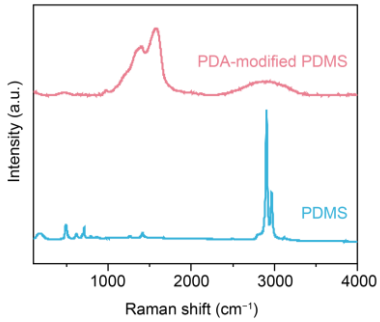

Figure S3. Raman spectra of bare PDMS and PDA-modified PDMS films.

170

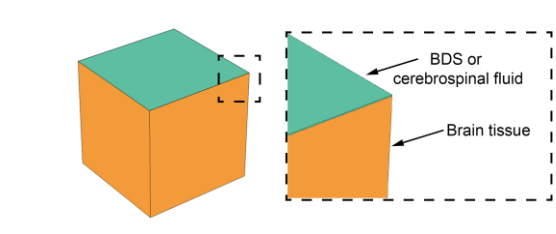

Figure S4. Schematic diagram of the model for finite element analysis.

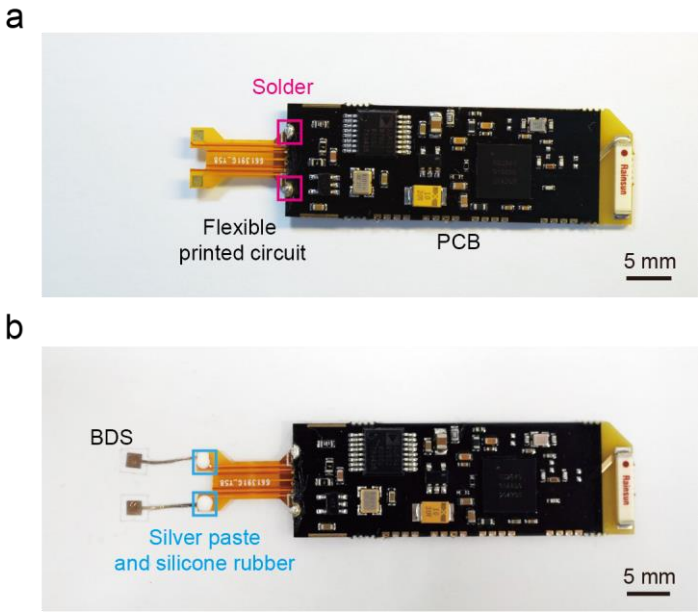

Figure S5. Photographs of BDS connected to the back-end device. a) Photograph of the connection between a two-channel flexible printed circuit and printed circuit board (PCB). b) Photograph of the connection between BDS and a two-channel flexible printed circuit.

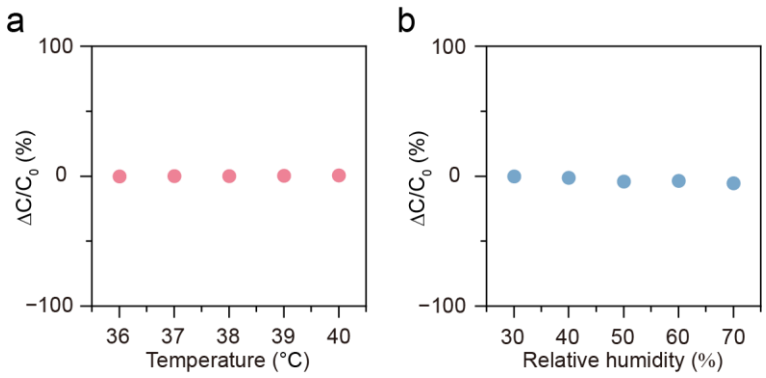

Figure S6. Capacitance monitoring under changing temperature and humidity. a) The capacitance changes with temperature varying from 36°C to 40°C. b) The capacitance changes with relative humidity varying from 30% to 70%.

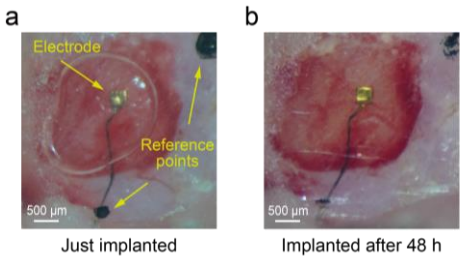

Figure S7. Photographs of the 300 × 300 μm PDA-modified electrode adhered to rat brain tissue. a) Electrode of the BDS just implanted. b) Electrode of BDS implanted after 48 h. Transparent poly(ethylene terephthalate) (PET) was used to seal the skull. The electrode remained in the same position of the rat brain after 48 h of free movement.

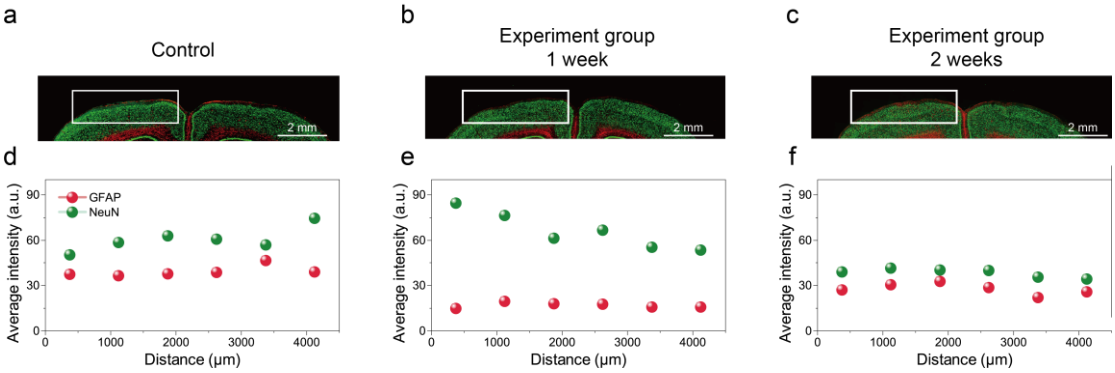

Figure S8. Biocompatibility of BDS implanted in the brains of rats. a-c) Fluorescence images of coronal brain sections without BDS (a) and with BDS implanted for 1 week (b) and 2 weeks (c). The sections were labeled with neurons (NeuN, green) and astrocytes (GFAP, red). The white frame indicated the BDS implanted area. d−f) The corresponding average fluorescence intensities of GFAP and NeuN in (a−c). The white frame was divided into six parts in the horizontal direction, and the fluorescence intensity of each part was calculated as the average value.

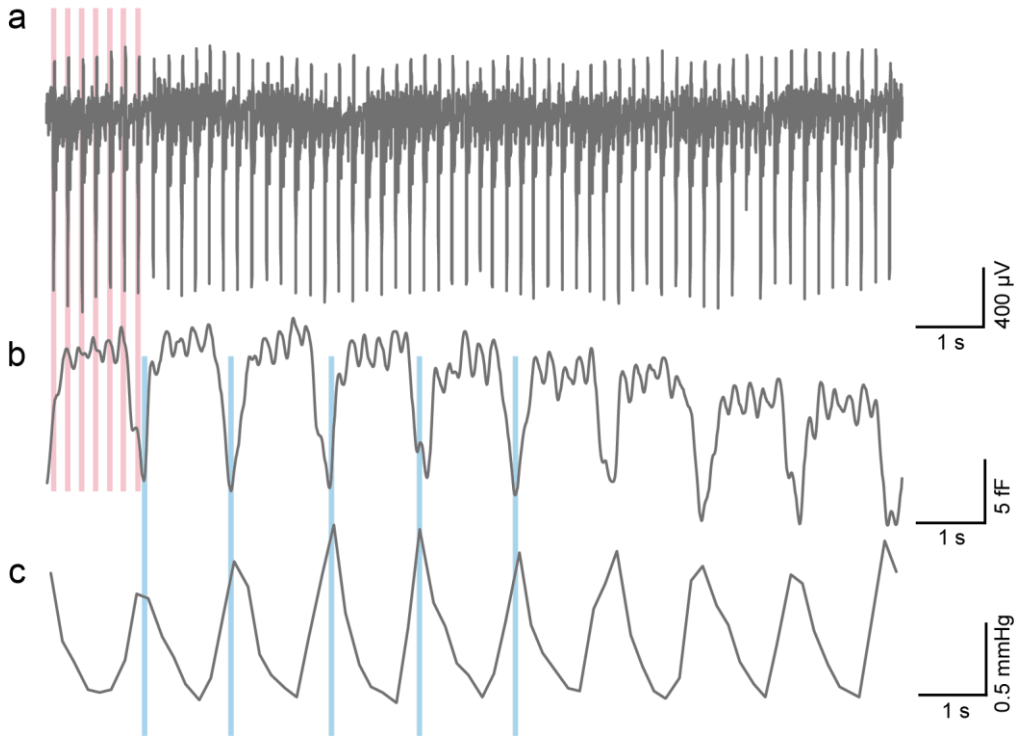

Figure S9. Simultaneous monitoring and comparison of electrocardiograph, end-tidal carbon dioxide wave and the brain deformation signals. a) Electrocardiograph of the anesthetized rat. b) Brain deformation signals monitored by BDS. c) End-tidal carbon dioxide wave of the anesthetized rat. The red line marked the QRS complexes of the electrocardiograph in (a) and the brain deformation signals induced by the heartbeat in (b), and the two signals coincided in the time domain. The blue line marked the end of the exhalation (the beginning of the inhalation) in (c) and the brain deformation signals induced by the respiration in (b), and the two signals coincided in the time domain.

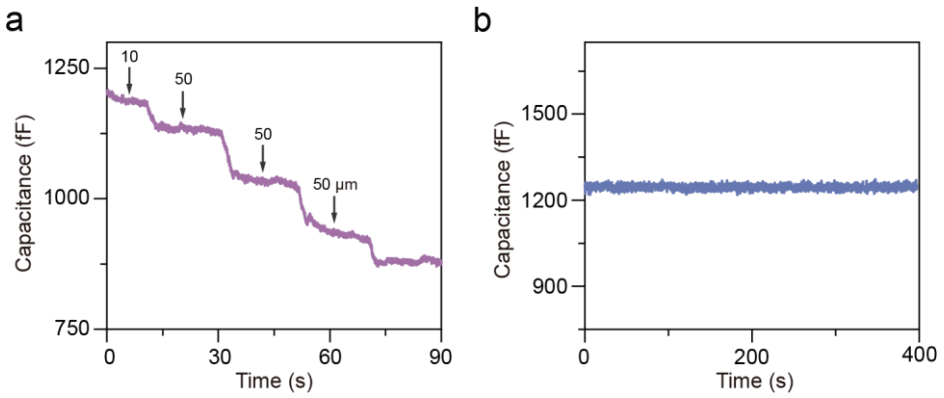

Figure S10. Sensing performances of the BDS placed on the rat skull. a) Capacitive response to the changed distance between the top and bottom electrodes by moving the top electrode. The bottom electrode was adhered to the rat skull, and the top electrode was fixed directly above the bottom electrode. b) Capacitive response of the BDS placed on the rat skull.

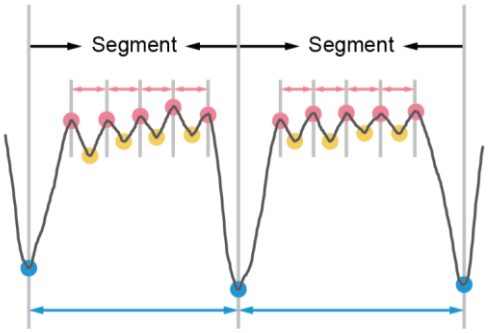

Figure S11. Illustration for the methodology used to decouple and differentiate the deformation signals. The signals were decoupled according to the frequencies. Firstly, the respiration-induced brain deformation valleys (blue dots) were extracted through spike detection according to the long time intervals. The intervals between the adjacent valleys (blue lines) were averaged to obtain the respiration-induced brain deformation cycle. Then, the horizontal coordinate was segmented with the respiration-induced brain deformation valleys. Finally, the spikes of heartbeat-induced brain deformation (red dots) were extracted by spike detection according to the short time intervals. The intervals between the adjacent spikes (red lines) were averaged to obtain the heartbeat-induced brain deformation cycle. The heartbeat-induced brain deformation valleys (yellow dots) were extracted through spike detection. The average of the heartbeat-induced brain deformation valleys is subtracted from the average of the heartbeat-induced brain deformation spikes within a segment to obtain the amplitude of brain deformation induced by heartbeat. The respiration-induced brain deformation amplitude was obtained by subtracting the heartbeat-induced brain deformation amplitude from the overall amplitude of the segment.

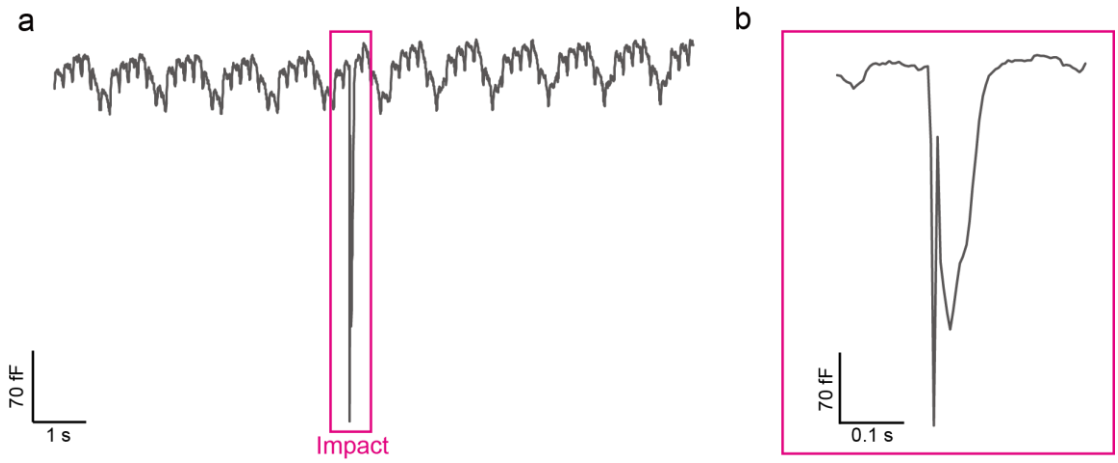

Figure S12. Continuous real-time monitoring of rat brain deformations. a) BDS capturing brain deformations induced by an incidental head impact of the living rat. b) Magnified trace of the transient brain deformation signal during impact. The impact site was the bottom of the rat's head.

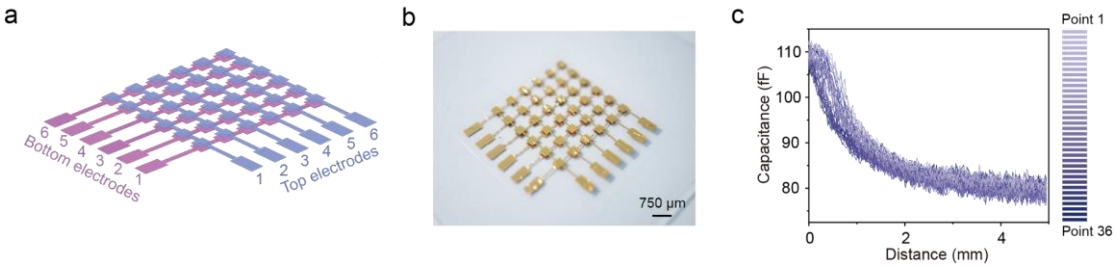

Figure S13. Design and basic performance of the brain deformation sensor array. a) Schematic of the 6 × 6 sensor array. b) Photograph of the 6 × 6 sensor array. c) Capacitive response of the 6 × 6 points of the sensor array.

Table S1. Comparison between BDS and existing imaging methods.

Methods	Temporal resolution (ms)	Continuous monitoring	Wearable capability	*Ref.*
X-ray	>83	No	No	*Comput. Tomogr.* **2009**, *3*, 403
MRI	>20	No	No	
PET	>5000	No	No	
BDS	**10**	**Yes**	**Yes**	**This work**